DOI 10.17816/transsyst201843154-163

© P. Sun[1,2], Q. Ge[1], Y. Li[1], X. Wang[1]
[1]Key Laboratory of Power Electronics and Electric Drive, Institute of Electrical Engineering, Chinese Academy of Sciences
[2]University of Chinese Academy of Sciences
(Beijing, China)

RESEARCH ON SPEED SENSORLESS CONTROL OF MAGLEV TRAIN WITH DOUBLE-END POWER SUPPLY

Background: The core technology of the stable operation of the maglev train is how to accurately obtain the train speed, position and motor angle information.

Aim: Using speed sensorless control method to estimate the speed and position of the maglev train.

Methods: In the double-end power supply mode of the maglev train, the principle of the extended back electromotive force (EEMF) of the AC motor is extended to the control of the long stator permanent magnet synchronous linear motor.

Results: The mathematical model for the power supply system of long-stator permanent magnet linear synchronous motor is established; based on the principle of EEMF of rotating motor, the EEMF observer is designed. The speed of the maglev train and the rotor angle are obtained by the method of phase locked loop (PLL).

Conclusion: Through the semi-physical simulation experiment, the speed sensorless control method is verified to be effective.

Keywords: Maglev train, long stator permanent magnet synchronous linear motor, speed sensorless control, extended electromotive force, double-end power supply

INTRODUCTION

The maglev train overcomes the friction of the vehicle with the rail, resulting in a significant increase in the speed of the rail train. The Germany TR system uses electromagnetic suspension technology (EMS). The Japanese MLX system uses electrodynamic suspension technology (EDS). The maglev of people transfer system in Shanghai is driven by the long-stator linear synchronous motor. The research content is also based on PMLSM mathematic model.

The core technology of the stable operation of the maglev train is how to accurately obtain the train speed, position and motor angle information. Usually at low speed, the speed and angle information can be determined by the sensor detecting the stator tooth and the positioning mark plate on the track and sent to the control system via the wireless transmission system. However, when the train is running at high speed, the long position information acquisition period cannot guarantee the control system to obtain accurate rotor field orientation angle and

Received: 20.07.2018. Revised: 13.08.2018. Accepted: 01.10.2018.
Transportation Systems and Technology. 2018;4(3):154-163

doi: 10.17816/transsyst201843154-163

train speed, resulting in poor control performance. Therefore, the effective solution is to use speed sensorless control algorithm. Real-time calculation of train speed and motor angle could ensure the stability control of the maglev train.

The speed sensorless technology of AC motor mainly includes direct calculation method, estimation method based on inductance change, back electromotive force integral method, extended back electromotive force method, extended Kalman filter method [1], model reference adaptive method [2], adaptive control, sliding mode observer [3], high frequency injection method [4, 5] and so on. These methods are for situations which single converter drives AC motor. The speed sensorless control method for long-stator linear synchronous motors in double-end power supply mode has not been reported in the works of literature.

The motor structure of the long-stator linear synchronous motor is quite different from the conventional rotary synchronous motor. The stator segments of the maglev train are laid along the track and the track parameters of the different stator are different. The inductance of the motor stator windings consists of multiple parts. The stator parameters of the stator windings in the area covered by the train differ from the uncovered portion. EEMF method is the use of motor armature current and voltage to calculate the flux and angle information. Compared with other methods, the method is simple and easy to implement, and has the strong robustness to the change of line parameters. Therefore, it is suitable for the control of the long-stator linear synchronous motor.

Compared with the single-end power supply, the mathematical model of maglev train with double-end power supply is more complicated. The input and output variables increase. If you want to directly calculate the EEMF, you need to design two observers. In this paper, the mathematic model of the converter and the long-stator linear synchronous motor is established. Then, combined with the EEMF theory proposed in [6], the EEMF principle of the AC motor is extended to the control of the long-stator linear synchronous motor. The observer of EEMF is designed. Finally, the semi-physical simulation experiments verify the effectiveness of the algorithm.

MATHEMATICAL MODEL OF LONG-STATOR LINEAR SYNCHRONOUS MOTOR WITH PARALLEL POWER SUPPLY

Maglev train in the high-speed operation uses double-end parallel power supply. Parallel power supply can provide greater drive current to meet the needs of high-speed operation; at the same time, it can reduce the output capacity of a single converter and ensure the reliability of power supply. The equivalent circuit of PMLSM with double-end power supply is shown in Fig. 1.

Received: 20.07.2018. Revised: 13.08.2018. Accepted: 01.10.2018.
Transportation Systems and Technology. 2018;4(3):154-163

doi: 10.17816/transsyst201843154-163

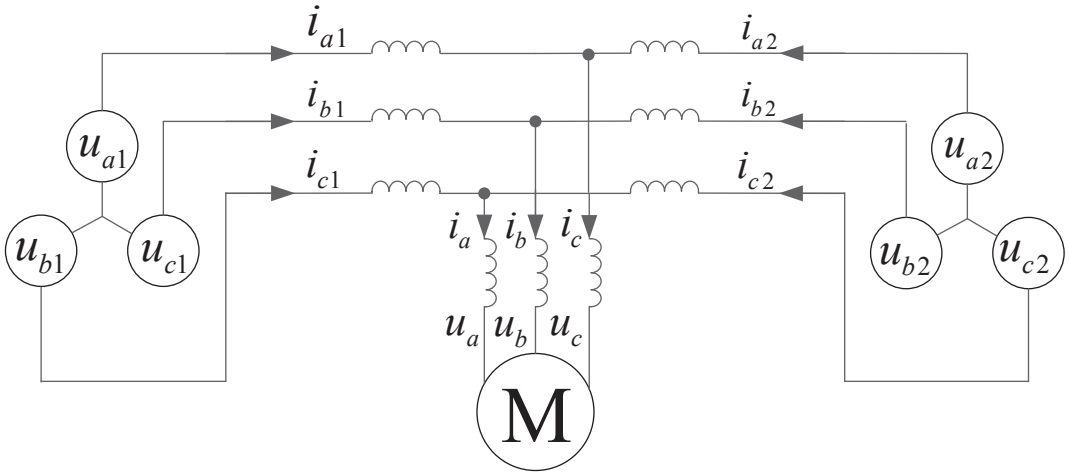

Fig. 1. Equivalent circuit of Long-Stator Linear Synchronous Motor with Double-End Power Supply

where u_{a1}, u_{b1}, u_{c1}, u_{a2}, u_{b2}, u_{c2} represent the output voltage of two converters; i_{a1}, i_{b1}, i_{c1}, i_{a2}, i_{b2}, i_{c2} represent the output current of two converters; u_a, u_b, u_c represent the voltage of stator windings; i_a, i_b, i_c represent the current of stator windings; M represent the long-stator linear synchronous motor.

Select the output current of each inverter as the state variables, the inverter output voltage as the input variables. The voltage equation of two converters and long-stator linear synchronous motor in the coordinate system is expressed as

$$(L_{k1}p + R_{k1})\begin{bmatrix} i_{\alpha 1} \\ i_{\beta 1} \end{bmatrix} = \begin{bmatrix} u_{\alpha 1} \\ u_{\beta 1} \end{bmatrix} - \begin{bmatrix} u_{\alpha} \\ u_{\beta} \end{bmatrix} \tag{1}$$

$$(L_{k1}p + R_{k1})\begin{bmatrix} i_{\alpha 1} \\ i_{\beta 1} \end{bmatrix} = \begin{bmatrix} u_{\alpha 1} \\ u_{\beta 1} \end{bmatrix} - \begin{bmatrix} u_{\alpha} \\ u_{\beta} \end{bmatrix}, \tag{2}$$

where L_{k1}, L_{k2} are the inductances of the feed cable; R_{k1}, R_{k2} are the resistances of the feed cable; $u_{\alpha 1}$, $u_{\beta 1}$ are the output voltage of the first converter; $i_{\alpha 1}$, $i_{\beta 1}$ are the output current of the first converter; $u_{\alpha 2}$, $u_{\beta 2}$ are the output voltage of the second converter; $i_{\alpha 2}$, $i_{\beta 2}$ are the output current of the second converter; u_{α}, u_{β} are the voltage of the linear motor; p is the differential operator. The equation of the long stator linear synchronous motor is shown in (3).

$$\begin{bmatrix} u_{\alpha} \\ u_{\beta} \end{bmatrix} = R\begin{bmatrix} i_{\alpha} \\ i_{\beta} \end{bmatrix} + \begin{bmatrix} pL_d & \omega_{re}(L_d - L_q) \\ -\omega_{re}(L_d - L_q) & pL_d \end{bmatrix}\begin{bmatrix} i_{\alpha} \\ i_{\beta} \end{bmatrix} + \tag{3}$$

Received: 20.07.2018. Revised: 13.08.2018. Accepted: 01.10.2018.
Transportation Systems and Technology. 2018;4(3):154-163

doi: 10.17816/transsyst201843154-163

$$+\{(L_d - L_q)(\omega_{re} i_d - i_q) + \omega_{re} K_E\}\begin{bmatrix} -\sin\theta_{re} \\ \cos\theta_{re} \end{bmatrix}$$

$$= R\begin{bmatrix} i_\alpha \\ i_\beta \end{bmatrix} + \begin{bmatrix} pL_d & \omega_{re}(L_d - L_q) \\ -\omega_{re}(L_d - L_q) & pL_d \end{bmatrix}\begin{bmatrix} i_\alpha \\ i_\beta \end{bmatrix} + Ex\begin{bmatrix} -\sin\theta_{re} \\ \cos\theta_{re} \end{bmatrix},$$

where L_d, L_q are the inductances of the direct-axis and quadrature-axis; R is the resistance of stator per-phase winding; ω_{re} is the electrical angular velocity; K_E is the coefficient of the EMF; θ_{re} is the rotor angle. The last term of (3) is the EEMF.

Substituting (3) into (1) and (2), the voltage equation as shown in (4) can be obtained. The equation describes the mathematical relationship between the first converter and the long-stator linear synchronous motor.

$$\begin{bmatrix} u_{\alpha 1} \\ u_{\beta 1} \\ u_{\alpha 2} \\ u_{\beta 2} \end{bmatrix} = \begin{bmatrix} L_{k1} + R_{k1} + L_d p & (L_d - L_q)\omega_{re} & L_d p & (L_d - L_q)\omega_{re} \\ -(L_d - L_q)\omega_{re} & L_{k1} + R_{k1} + L_d p & -(L_d - L_q)\omega_{re} & L_d p \\ L_d p & (L_d - L_q)\omega_{re} & L_{k2} + R_{k2} + L_d p & (L_d - L_q)\omega_{re} \\ -(L_d - L_q)\omega_{re} & L_d p & -(L_d - L_q)\omega_{re} & L_{k2} + R_{k2} + L_d p \end{bmatrix} \times$$

$$\times \begin{bmatrix} i_{\alpha 1} \\ i_{\beta 1} \\ i_{\alpha 2} \\ i_{\beta 2} \end{bmatrix} + Ex\begin{bmatrix} -\sin\theta \\ \cos\theta \\ -\sin\theta \\ \cos\theta \end{bmatrix} \qquad (4)$$

DESIGN THE OBSERVER OF EEMF

The current of the long-stator linear synchronous motor with double-end power supply is equal to the sum of the current of the two converters. The relationship between them is shown as follows

$$\begin{bmatrix} i_\alpha \\ i_\beta \end{bmatrix} = \begin{bmatrix} i_{\alpha 1} \\ i_{\beta 1} \end{bmatrix} + \begin{bmatrix} i_{\alpha 2} \\ i_{\beta 2} \end{bmatrix}, \qquad (5)$$

where i_α, i_β are the current of the motor.

The first two equations in (4) are symmetrical with the latter two equations, and both include the EEMF terms. Substituting (5) into (4) could obtain a new voltage equation.

Received: 20.07.2018. Revised: 13.08.2018. Accepted: 01.10.2018.
Transportation Systems and Technology. 2018;4(3):154-163

doi: 10.17816/transsyst201843154-163

$$\begin{bmatrix}(L_{k1}+L_d)pi_{\alpha1}+L_d pi_{\alpha2}\\(L_{k1}+L_d)pi_{\beta1}+L_d pi_{\beta2}\end{bmatrix}= \\ =\begin{bmatrix}u_{\alpha1}\\u_{\beta1}\end{bmatrix}-\begin{bmatrix}R_{k1}i_{\alpha1}\\R_{k1}i_{\beta1}\end{bmatrix}-\begin{bmatrix}Ri_{\alpha}\\Ri_{\beta}\end{bmatrix}-\begin{bmatrix}(L_d-L_q)\omega i_{\beta}\\-(L_d-L_q)\omega i_{\alpha}\end{bmatrix}+\begin{bmatrix}Ex\sin\theta\\-Ex\cos\theta\end{bmatrix} \quad (6)$$

In (6), both the current differential terms of the first and second converter are included. The complex formula adds difficulty to designing the observer. Therefore, it is necessary to eliminate the current differential term of one converter.

According to the voltage equations (1) and (2), the relationship between the voltage and current of the two converters can be obtained as shown in (7).

$$\begin{bmatrix}pi_{\alpha2}\\pi_{\beta2}\end{bmatrix}=\begin{bmatrix}(u_{\alpha2}-u_{\alpha1}+R_{k1}i_{\alpha1}-R_{k2}i_{\alpha2}+L_{k1}pi_{\alpha1})/L_{k2}\\(u_{\beta2}-u_{\beta1}+R_{k1}i_{\beta1}-R_{k2}i_{\beta2}+L_{k1}pi_{\beta1})/L_{k2}\end{bmatrix} \quad (7)$$

According to (6) and (7), the estimated value of the EEMF can be obtained by the action of the PI regulator by the difference between the current calculated value and the current measured value. The mathematical expression of the extended back EMF observer can be obtained.

$$\begin{aligned}&[(L_{k1}L_{k2}+L_{k2}L_d+L_{k1}L_d)p+(L_dR_{k1}+L_{k2}R_{k1}+L_{k2}R)]\hat{i}_{\alpha1}\\&=(L_{k2}+L_d)u_{\alpha1}-L_du_{\alpha2}+(L_dR_{k2}-L_{k2}R)i_{\alpha2}-\\&-L_{k2}(L_d-L_q)\hat{\omega}(i_{\beta1}+i_{\beta2})+L_{k2}\frac{K_Ps+K_I}{s}(i_{\alpha1}-\hat{i}_{\alpha1})\end{aligned} \quad (8)$$

$$\begin{aligned}&[(L_{k1}L_{k2}+L_{k2}L_d+L_{k1}L_d)p+(L_dR_{k1}+L_{k2}R_{k1}+L_{k2}R)]\hat{i}_{\beta1}\\&=(L_{k2}+L_d)u_{\beta1}-L_du_{\beta2}+(L_dR_{k2}-L_{k2}R)i_{\beta2}+\\&+L_{k2}(L_d-L_q)\hat{\omega}(i_{\alpha1}+i_{\alpha2})-L_{k2}\frac{K_Ps+K_I}{s}(i_{\beta1}-\hat{i}_{\beta1}),\end{aligned} \quad (9)$$

where $\hat{i}_{\alpha1}$, $\hat{i}_{\beta1}$ are the measured values of the first converter current.

According to the mathematical expression of the EEMF observer, the EEMF observer shown in Fig. 2 can be designed.

Among them,

$$A=L_{k1}L_{k2}+L_{k2}L_d+L_{k1}L_d$$
$$B=L_dR_{k1}+L_{k2}R_{k1}+L_{k2}R$$

Received: 20.07.2018. Revised: 13.08.2018. Accepted: 01.10.2018.
Transportation Systems and Technology. 2018;4(3):154-163

doi: 10.17816/transsyst201843154-163

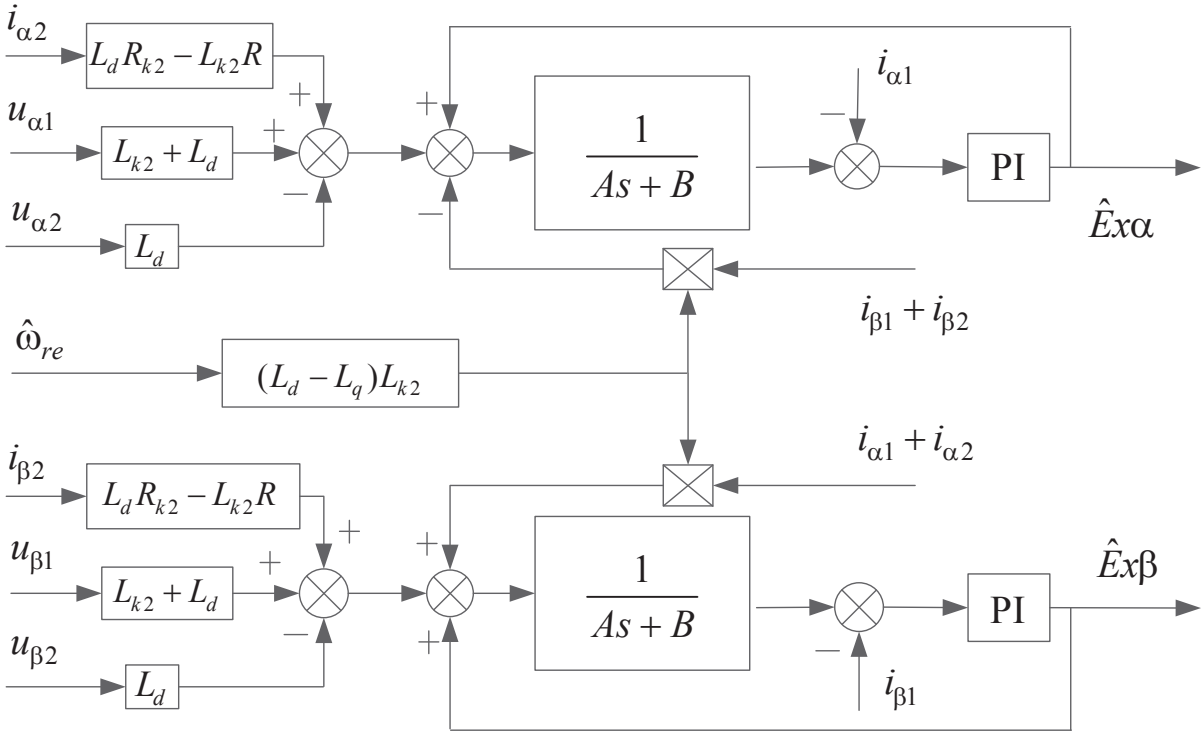

Fig. 2. Diagram of EEMF Observer

PHASE LOCKED LOOP TECHNOLOGY

The two quadrature components of the EEMF have been obtained in the previous section. According to the second section, it can be seen that the EEMF contains the rotor position information. In this paper, the principle of the phase locked loop is used to extract the rotor angle information of the long-stator linear synchronous motor. The principle of PLL is expressed as

$$\ddot{A}\theta = Ex(-\sin\theta)\cos\hat{\theta} + Ex\cos\theta * \sin\hat{\theta} = Ex\sin(\hat{\theta} - \theta) \qquad (10)$$

Among them, $\Delta\theta$ is the angle difference; $\hat{\theta}$ is the estimated angle of linear motor; θ is the actual angle of the linear motor.

Equation (10) is defined as the tracking error function. When the tracking error is equal to zero, the actual angle θ and the estimated angle are approximately equal.

The angle difference after the PI regulator processing can be treated as the rotor electrical angular velocity; the rotor is obtained by the integration of the angular velocity. The principle of PLL is shown in Fig. 3.

Received: 20.07.2018. Revised: 13.08.2018. Accepted: 01.10.2018.
Transportation Systems and Technology. 2018;4(3):154-163

doi: 10.17816/transsyst201843154-163

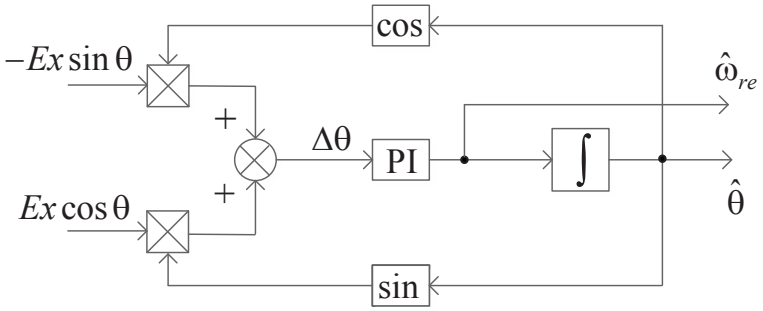

Fig. 3. Diagram of Phase-lock Loop

SEMI-PHYSICAL SIMULATION RESULTS

In order to verify the feasibility and effectiveness of the speed sensorless control algorithm proposed in this paper, the experimental study was carried out on the high-speed maglev semi-physical simulation platform. The simulation platform is shown in Fig. 4.

Fig. 4. Experimental platform of maglev train semi-physical simulation

The goal of the experiment is to make the train with five groups achieve the maximum speed of 430 km/h acceleration and deceleration process.

Fig. 5 is the experimental comparison of the estimated speed and actual speed. The whole running process lasted 380 seconds, the maximum speed of maglev train reached 430km/h. It can be seen from the velocity curve that the estimated speed of the speed sensorless algorithm is basically consistent with the actual speed.

Fig. 6 is the experimental curve of the EEMF. When the train is running at low speed, the EEMF is affected by the current, so it has some chattering. When

Received: 20.07.2018. Revised: 13.08.2018. Accepted: 01.10.2018.
Transportation Systems and Technology. 2018;4(3):154-163

doi: 10.17816/transsyst201843154-163

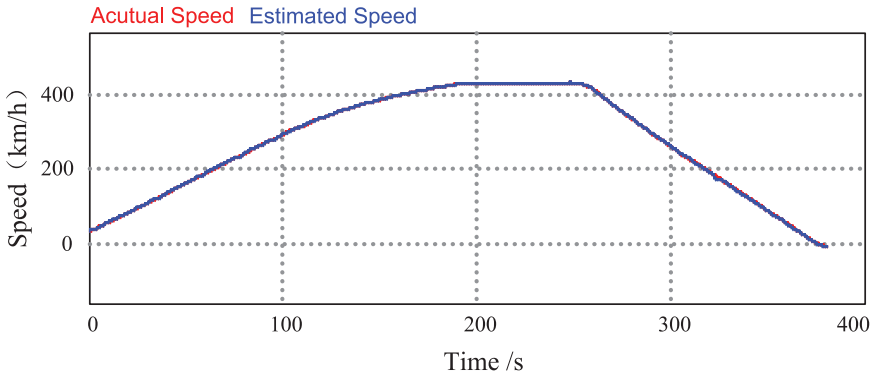

Fig. 5. Comparison of actual speed and estimated speed

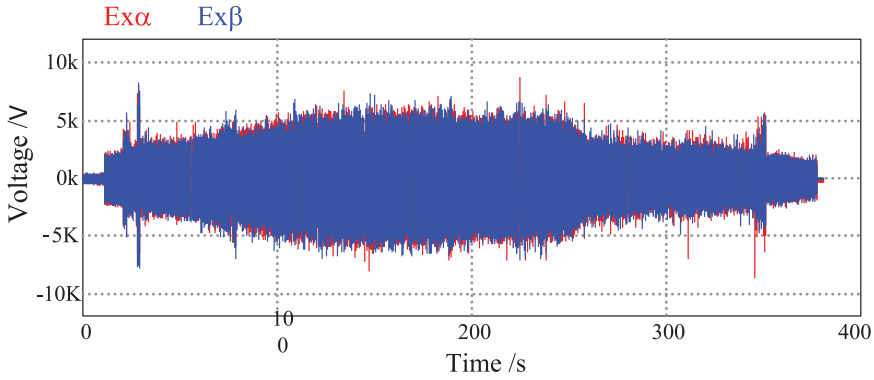

Fig. 6. Experimental results of EEMF

the train is running at high speed, the EEMF is stabilized. It can be seen from the figure that the EEMF is consistent with the train speed variation.

According to the comparison between the actual angle and the estimated angle in Fig. 7 and the partial magnification, it can be seen that the angle calculated by the speed sensorless is substantially coincident with the true angle.

The switching of the stator segments in the train operation is achieved by a two-step method. When the stator segment is switching, the stator voltage and current on one side are reduced, resulting in a decrease of the EEMF, so the calculated angle is not accurate. As shown in the first picture in Fig. 8. But the stator current and voltage on the other side do not change. The result of the calculation using the converter parameters of the other side is still accurate. As shown in the second picture in Fig. 8.

In order to obtain an accurate angle in the operation of the train, the angle calculated from the B-side converter data will be used when the A-side stator changing segment, and other times still using the A-side of the converter data to calculate the angle.

Through the use of the above method, the maglev train can be stably controlled in the two-step mode.

Received: 20.07.2018. Revised: 13.08.2018. Accepted: 01.10.2018.
Transportation Systems and Technology. 2018;4(3):154-163

doi: 10.17816/transsyst201843154-163

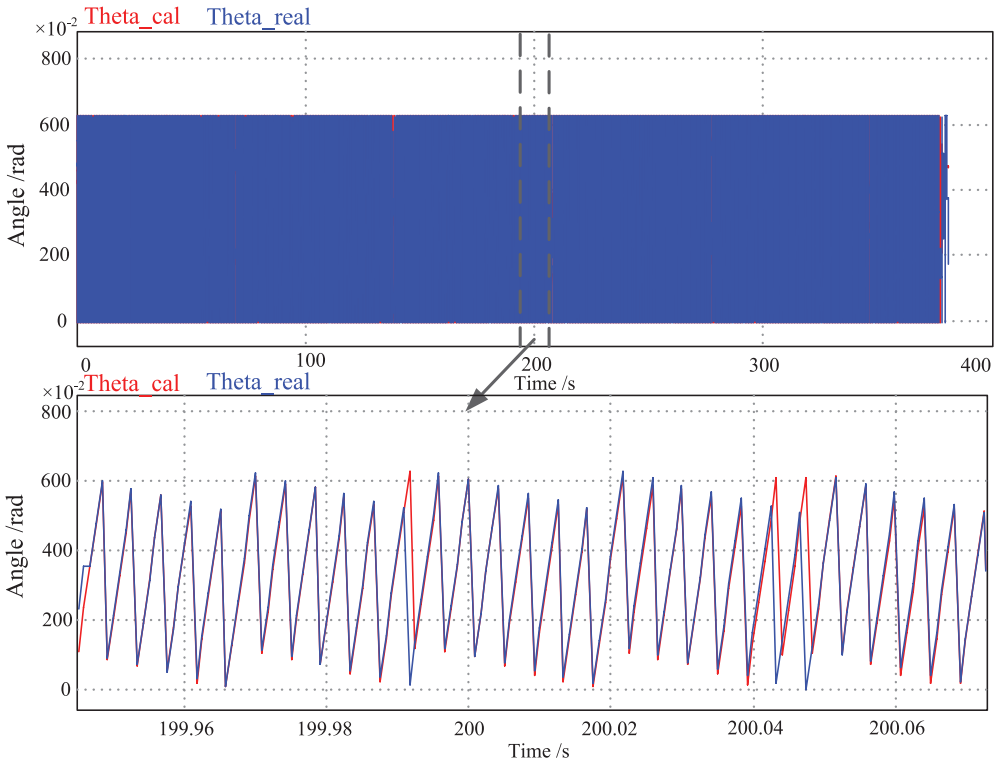

Fig. 7. Comparison of actual angle and estimated angle

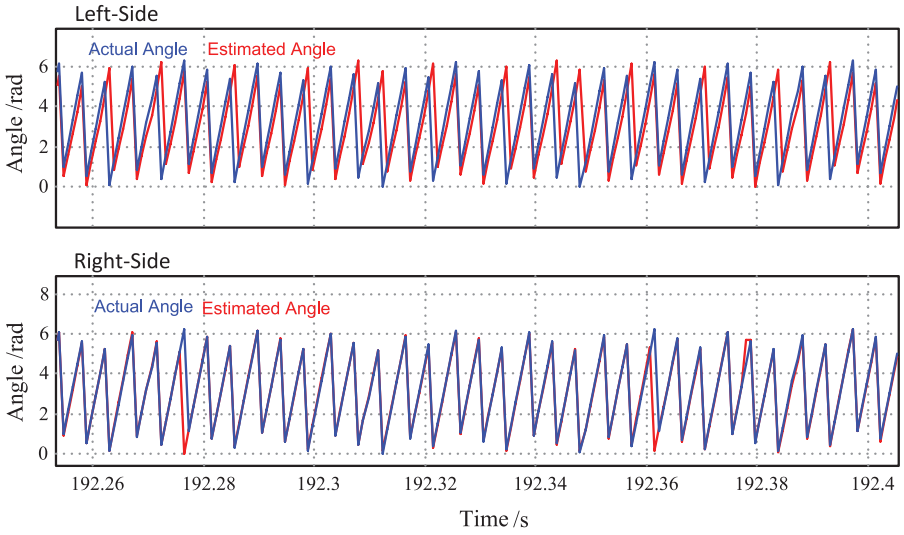

Fig. 8. The angle differences between both sides of the track when stator changing step

CONCLUSION

In this paper, a mathematical model of the long-stator linear synchronous motor in double-end power supply mode is established. Based on the basic principle of extended back EMF, an observer of EEMF is established. In this paper, the design of the observer, involving only α-β coordinate system transformation, does

Received: 20.07.2018. Revised: 13.08.2018. Accepted: 01.10.2018.
Transportation Systems and Technology. 2018;4(3):154-163

doi: 10.17816/transsyst201843154-163

not involve the d-q coordinate system transformation, reduction the use of the estimated angle of the link, so that the entire control system is more stable. From the results of the semi-physical simulation, the design of the speed sensorless algorithm can realize the effective control of the high-speed operation of the maglev train, which is of great value to the practical application of the high-speed maglev train.

References

1. Yin Z, Xiao L, Sun X, et al. A Speed Estimation Method of Fuzzy Extended Kalman Filter for Induction Motors Based on Particle Swarm Optimization. *Transactions of China Electrotechnical Society*. 2016;31:55-65.
2. Angelo A, Maurizio C, Marcello P, et al. Closed-Loop MRAS Speed Observer for Linear Induction Motor Drives. *IEEE Transactions on Industry Applications.* 2015;51(3):2279-2290. doi: 10.1109/tia.2014.2375377
3. Zhao L, Huang J, Liu H, et al. Second-Order Sliding Mode Observer with Online Parameter Identification for Sensorless Induction Motor Drives. *IEEE Transactions on Industrial Electronics*. 2014;61(10):5280-5289. doi: 10.1109/tie.2014.2301730
4. Li Y, Huang S, Xu Q, et al. Sensorless Control of Permanent Magnet Synchronous Motor Based on High Frequency Voltage Signal Injection. *Transactions of China Electrotechnical Society*, 2013;28:326-330.
5. Yoon TM, Sim HW, Lee JS, et al. A Simplified Method to Esimate the Rotor Position Using the High Frequency Voltage Signal Injection. *IEEE Applied Power Electronics Conference and Exposition (APEC 2014)*. 2014 March; p. 2453-2458. doi: 10.1109/apec.2014.6803647
6. Zhiqian C, Tomita M, Doki S, et al. An Extended Electromotive Force Model for Sensorless Control of Interior Permanent Magnet Synchronous Motors. *IEEE Transactions on Industrial Electronics.* 2003;50(2):288-295. doi: 10.1109/tie.2003.809391

Information about the authors:
Pengkun Sun, graduate student; Address: No.6 Beiertiao, Zhongguancun, Beijing, China
ORCID: 0000-0001-8958-2606;
E-mail: sunpengkun@mail.iee.ac.cn

Qiongxuan Ge, Doctor of Philosophy
E-mail: gqx@mail.iee.ac.cn

Yaohua Li, Doctor of Philosophy;
E-mail: yhli@mail.iee.ac.cn

Xiaoxin Wang, Master Degree;
E-mail: wxxhit@mail.iee.ac.cn

To cite this article:
Sun P, Ge Q, Li Y, Wang X. Research on Speed Sensorless Control of Maglev Train with Double-End Power Supply. *Transportation Systems and Technology.* 2018;4(3):154-163. doi: 10.17816/transsyst201843154-163

Received: 20.07.2018. Revised: 13.08.2018. Accepted: 01.10.2018.
Transportation Systems and Technology. 2018;4(3):154-163

doi: 10.17816/transsyst201843154-163